

Centaurus A as a point source of Ultra-High Energy Cosmic Rays

Hang Bae Kim*

*Department of Physics and The Research Institute of Natural Science,
Hanyang University, Seoul 133-791, Korea*

We probe the possibility that Centaurus A (Cen A) is a point source of ultra-high energy cosmic rays (UHECR) observed by PAO, through the statistical analysis of the arrival direction distribution. For this purpose, we set up the Cen A dominance model for the UHECR sources, in which Cen A contributes the fraction f_C of the whole UHECR with energy above 5.5×10^{19} eV and the isotropic background contributes the remaining $1 - f_C$ fraction. The effect of the intergalactic magnetic fields on the bending of the trajectory of Cen A originated UHECR is parameterized by the gaussian smearing angle θ_s . For the statistical analysis, we adopted the correlational angular distance distribution (CADD) for the reduction of the arrival direction distribution, and the Kuiper test to compare the observed and the expected CADDs. Using CADD, we identify the excess of UHECR in the Cen A direction and fit the CADD of the observed PAO data by varying two parameters f_C and θ_s of the Cen A dominance model. The best-fit parameter values are $f_C \approx 0.1$ (The corresponding Cen A fraction observed at PAO is $f_{C,PAO} \approx 0.15$, that is, about 10 out of 69 UHECR.) and $\theta_s = 5^\circ$ with the maximum probability $P_{\max} = 0.29$. Considering the uncertainty concerning the assumption of isotropic background in the Cen A dominance model, we extend the viable parameter ranges to the 2σ band, $0.09 \lesssim f_{C,PAO} \lesssim 0.25$ and $0^\circ \lesssim \theta_s \lesssim 20^\circ$. This result supports the existence of a point source extended by the intergalactic magnetic fields in the direction of Cen A. If Cen A is actually the source responsible for the observed excess of UHECR, the average deflection angle of the excess UHECR implies the order of 10 nG intergalactic magnetic field in the vicinity of Cen A.

PACS numbers: 98.70.Sa

Keywords: ultra high energy cosmic rays, Centaurus A, active galactic nuclei

* hbkim@hanyang.ac.kr

I. INTRODUCTION

The origin of the ultra-high energy cosmic rays (UHECR) is a long-standing puzzle [1]. The recent confirmation of the Greisen-Zatsepin-Kuzmin (GZK) suppression in the cosmic ray energy spectrum [2–4] implies that UHECR with energies above the GZK cutoff, $E_{\text{GZK}} \sim 4 \times 10^{19}$ eV, mostly come from relatively close extragalactic sources within the GZK radius $r_{\text{GZK}} \sim 100$ Mpc. Furthermore, UHECR with these energies are expected not to be strongly affected by the galactic or extragalactic magnetic field, so that their arrival directions keep some correlation with the source distribution and can be used to trace the sources of UHECR. Recently Pierre Auger Observatory (PAO) released the updated UHECR data with energy $E \geq 5.5 \times 10^{19}$ eV [5]. These data can be used for tracing the distribution of UHECR sources through the statistical analysis of the arrival direction distribution. Beginning with the report of the correlation between UHECR and active galactic nuclei (AGN) by the PAO collaboration [5–7], several attempts were made to identify the UHECR sources. Most attempts aimed to test the plausibility of a certain kind of high energy astrophysical objects whose number ranges from a few to a few hundred [8–14]. In this paper, we aim to test the other extreme possibility that a single dominating source is responsible for the large part of observed UHECR.

The most mentioned candidates for a strong UHECR source are Centaurus A (Cen A) and Messier 87 in Virgo cluster, which are active galaxies very close to us. Many people suggested that Cen A might be the source of UHECR [15–22]. Cen A is located in the southern sky, near the center of the exposure region of the PAO experiment. Therefore, the PAO data provide the best chance for checking whether Cen A is a strong source of UHECR. Actually, the correlation of UHECR with AGN was strengthened by many UHECR observed around Cen A. On the contrary, the number of UHECR around M87 is smaller than the expected one considering its distance, weakening the claimed AGN correlation. Our purpose is to quantify the Cen A contribution in the observed UHECR by PAO and thus try to establish the existence of a point source in the Cen A direction.

For a single dominating source to be able to explain the large portion of UHECR data, the intergalactic magnetic fields must play a significant role, spreading UHECR over the large region of the sky around the source. Unfortunately, our knowledge about the intergalactic magnetic fields is rather poor yet. Modeling the intergalactic magnetic fields and testing it has its own uncertainty. For this reason, we choose a different and simpler strategy. We parameterize the effect of intergalactic magnetic fields on the deflection of UHECR trajectory by the gaussian spreading of UHECR arrival directions around the sources. In addition, we also need to consider the contribution from other sources to explain the whole set of observed UHECR arrival directions. For this purpose, we introduce one more parameter measuring the fraction of Cen A contribution to observed UHECR. Then we search for the values of two parameters with which the observed UHECR arrival directions can be plausibly explained through the statistical comparison of the arrival direction distributions.

Statistical comparison of the arrival direction distributions can be done in many different ways. In Ref. [23, 24], we developed the new statistical test methods, whose basic idea is that the two-dimensional distribution of arrival directions is reduced to the one-dimensional probability distributions, which can be compared by using the well-known Kolmogorov-Smirnov test or its variants. We proposed a few reduced one-dimensional distributions suitable for the test of correlation between the UHECR arrival directions and the point sources. Among them, we adopt the correlational angular distance distribution method and

the flux-exposure value distribution method. These methods will be briefly described in Sec. III.

This paper is organized as follows. In section II, we explain the Cen A dominance model for the UHECR sources and the details needed for the Monte-Carlo simulations of UHECR arrival directions. In section III, we briefly introduce our statistical methods for comparing two arrival direction distributions. In Section IV, the results of our analysis are presented. We give a few discussions on the results and conclude in section V.

II. THE SINGLE DOMINATING SOURCE MODEL FOR UHECR

We examine the plausibility of the idea that the Cen A is the dominant sources of UHECR through the statistical analysis of the arrival direction distribution of UHECR. For more definite interpretation of our analysis, we need to solidify the UHECR source model with the Cen A dominance and the methods adopted for statistical analysis. In this section, we describe the details of the Cen A dominance model for UHECR sources.

Cen A is located at $\alpha = 201.37^\circ$, $\delta = -43.02^\circ$ in the equatorial coordinates and the distance is estimated to be $3 - 5$ Mpc [25]. We consider Cen A as a smeared point sources of UHECR. This is mainly to incorporate the fact that the trajectories of UHECR can be bent by intervening magnetic fields. We may model the intervening galactic and extragalactic magnetic fields between Cen A and the earth. But, it would involve large arbitrariness due to our lack of knowledge on extragalactic magnetic fields. Instead of such detailed modeling of magnetic fields, we simply assume that Cen A has a gaussian flux distribution on the sky with a certain angular width θ_s , so that the effect of magnetic fields is measured through the parameter θ_s , called the smearing angle. Then the UHECR flux at a direction $\hat{\mathbf{r}}$ contributed by Cen A can be written as

$$F_{\text{CA}}(\hat{\mathbf{r}}) = \overline{F}_{\text{CA}} \frac{\exp[-(\theta_j(\hat{\mathbf{r}})/\theta_s)^2]}{N(\theta_s)}, \quad (1)$$

where \overline{F}_{CA} is the averaged flux of Cen A, $\theta(\hat{\mathbf{r}}) = \cos^{-1}(\hat{\mathbf{r}} \cdot \hat{\mathbf{r}}_{\text{CA}})$ is the angle between the direction $\hat{\mathbf{r}}$ and Cen A, and $N(\theta_s) = (1/4\pi) \int d\Omega \exp[-(\theta(\hat{\mathbf{r}})/\theta_s)^2]$ is the normalization of smearing function. For small θ_s , $N(\theta_s) \approx \theta_s^2/4$ and for large θ_s , $N(\theta_s) \approx 1$. For the small smearing angle θ_s , the average deflection angle is $\langle \theta \rangle \equiv \int \theta e^{-(\theta/\theta_s)^2} d\Omega / \int e^{-(\theta/\theta_s)^2} d\Omega \approx \theta_s$, and $\Delta\theta \equiv \sqrt{\langle \theta^2 \rangle - \langle \theta \rangle^2} \approx \theta_s/2$.

Though Cen A can be a dominant source of UHECR, it is very unlikely that Cen A is the only source of UHECR. We need to consider the contribution from other distributed sources. We consider, for the sake of simplicity, that a certain fraction of UHECR are originated from Cen A, while the remaining fraction of them are from the isotropically distributed background contributions. Then, the expected flux at a give arrival direction $\hat{\mathbf{r}}$ is given by the sum of two contributions,

$$F(\hat{\mathbf{r}}) = F_{\text{CA}}(\hat{\mathbf{r}}) + F_{\text{ISO}}. \quad (2)$$

Now we define the Cen A fraction f_C to be

$$f_C = \frac{\overline{F}_{\text{CA}}}{\overline{F}_{\text{CA}} + F_{\text{ISO}}}. \quad (3)$$

The UHECR flux can be written as

$$F(\hat{\mathbf{r}}) = f_C \bar{F} \frac{\exp[-(\theta(\hat{\mathbf{r}})/\theta_s)^2]}{N(\theta_s)} + (1 - f_C) \bar{F}, \quad (4)$$

where $\bar{F} = \bar{F}_C + F_{\text{ISO}}$. Out of three parameters \bar{F}_C , F_{ISO} , and θ_s , the Cen A fraction f_C and the smearing angle θ_s are treated as the free parameters of the model, while the average flux \bar{F} is fixed by the total number of UHECR events.

To do the simulation for the observed arrival directions of UHECR, we also need to take into account the efficiency of the detector as a function of the arrival direction. It depends on the location and the characteristics of the detector array. Here we consider only the geometric efficiency which is determined by the location and the zenith angle cut of the detector array. Then the exposure function $h(\hat{\mathbf{r}})$ depends only on the declination δ ,

$$h(\delta) = \frac{1}{\pi} [\sin \alpha_m \cos \lambda \cos \delta + \alpha_m \sin \lambda \sin \delta], \quad (5)$$

where λ is the latitude of the detector array, θ_m is the zenith angle cut, and

$$\alpha_m = \begin{cases} 0, & \text{for } \xi > 1, \\ \pi, & \text{for } \xi < -1, \\ \cos^{-1} \xi, & \text{otherwise} \end{cases} \quad \text{with } \xi = \frac{\cos \theta_m - \sin \lambda \sin \delta}{\cos \lambda \cos \delta}.$$

The expected flux at the detector array is proportional to $F(\hat{\mathbf{r}})h(\hat{\mathbf{r}})$. We also note that the Cen A fraction f_C is the fraction of Cen A contribution over the whole sky. It is in general different from the fraction of Cen A contribution within the sky covered by a given detector array, because the latter is masked by the exposure function. We denote the latter, e.g. for PAO, by $f_{C,\text{PAO}}$ to distinguish it from the former.

III. STATISTICAL COMPARISON OF TWO ARRIVAL DIRECTION DISTRIBUTIONS

We now turn to the statistical methods to measure the plausibility of the Cen A dominance model. In Refs. [23, 24], we developed the simple comparison method for the UHECR arrival direction distributions, where the two-dimensional UHECR arrival direction distributions on the sphere is reduced to one-dimensional probability distributions of some sort, so that they can be compared by using the standard Kolmogorov-Smirnov (KS) test or its variants. In this paper, we adopt the reduction methods called the correlational angular distance distribution (CADD) and the flux-exposure value distribution (FEVD). For a detailed explanation on these methods, see Refs. [23, 24]. Here we present briefly the basic ideas of these distributions and how to calculate the probability measuring the plausibility.

- *Correlational Angular Distance Distribution* This is the distribution of the angular distances of all pairs UHECR arrival directions and the point source directions:

$$\text{CADD} : \{\cos \theta_{ij'} \equiv \hat{\mathbf{r}}_i \cdot \hat{\mathbf{r}}'_j \mid i = 1, \dots, N; j = 1, \dots, M\}, \quad (6)$$

where $\hat{\mathbf{r}}_i$ are the UHECR arrival directions, $\hat{\mathbf{r}}'_j$ are the point source directions, and N and M are their total numbers, respectively.

- *Flux Exposure Value Distribution* At a given arrival direction, the expected flux value is the product of the UHECR flux expected from the UHECR source model and the exposure function of the detector at that direction. FEVD is the distribution of expected flux values at UHECR arrival directions:

$$\text{FEVD} : \{F_i \equiv F(\hat{\mathbf{r}}_i)h(\hat{\mathbf{r}}_i) \mid i = 1, \dots, N\}, \quad (7)$$

where $\hat{\mathbf{r}}_i$ are the UHECR arrival directions, N is the total numbers of UHECR, $F(\hat{\mathbf{r}}_i)$ and $h(\hat{\mathbf{r}}_i)$ are the UHECR flux and the exposure function, respectively.

From the given point source set and the UHECR arrival direction data set, we can get CADD and FEVD. Then, we can apply KS test or its variants such as Kuiper test and Anderson-Darling test to compare two CADDs or two FEVDs, one from the observed UHECR data set and the other from the expected (simulated) UHECR data set from the model under consideration. In this analysis, we use Kuiper (KP) test because its sensitivity is found to be most appropriate for our purpose and the probability function of its statistic is available in analytic form. The KP test is based on the cumulative probability distribution (CPD), $S_N(x) = \int^x p(x')dx'$ and the KP statistic is the sum of maximum difference above and below two CPDs,

$$D_{\text{KP}} = \max_x [S_{N_1}(x) - S_{N_2}(x)] + \max_x [S_{N_2}(x) - S_{N_1}(x)]. \quad (8)$$

From the KP statistic D_{KP} , the probability that CADD/FEVD of the observed data is obtained from the model under consideration can be estimated using the Monte-Carlo simulations in general. For the KP statistic D_{KP} , when the data in the distribution are all independently sampled, the following approximation formula is available:

$$P(D_{\text{KP}}|N_e) = Q_{\text{KP}}([\sqrt{N_e} + 0.155 + 0.24/\sqrt{N_e}]D_{\text{KP}}), \quad (9)$$

where $Q_{\text{KP}}(\lambda) = 2 \sum_{j=1}^{\infty} (4j^2\lambda^2 - 1)e^{-2j^2\lambda^2}$ and $N_e = N_1 N_2 / (N_1 + N_2)$ is the effective number of data. For FEVD, the number of data in the distribution is same as the number of UHECR data. For CADD, the number of data in the distribution is the number of UHECR data times the number of point sources. Therefore, for a single source case, the number of data in the distribution CADD and FEVD is same as the number of UHECR data. This means that the data in CADD and FEVD are all independent, and we can use the formula (9) for both CADD and FEVD for a single source model. Now, $N_1 = N_O$, the number of observed UHECR data and $N_2 = N_S$, the number of mock UHECR data. We can make the expected distribution more accurate by increasing the number of mock data N_2 . In the limit $N_2 \rightarrow \infty$, the effective number of data is simply $N_e = N_O$.

IV. THE RESULTS OF STATISTICAL TESTS

For the observed UHECR data set, we use the UHECR data released by PAO in 2010 [5]. The released data set contains 69 UHECR with energy higher than 5.5×10^{19} eV. The PAO site has the latitude $\lambda = -35.20^\circ$ and the zenith angle cut of the released data is $\theta_m = 60^\circ$. The arrival direction distribution of the released PAO data is shown in Fig. 1. The locations of Cen A and M87 are also marked for reference. For the correlation test between the UHECR arrival directions and the astrophysical objects, the choice of the energy cut can be crucial. For low energy UHECR, the effects of intergalactic magnetic fields may be so strong

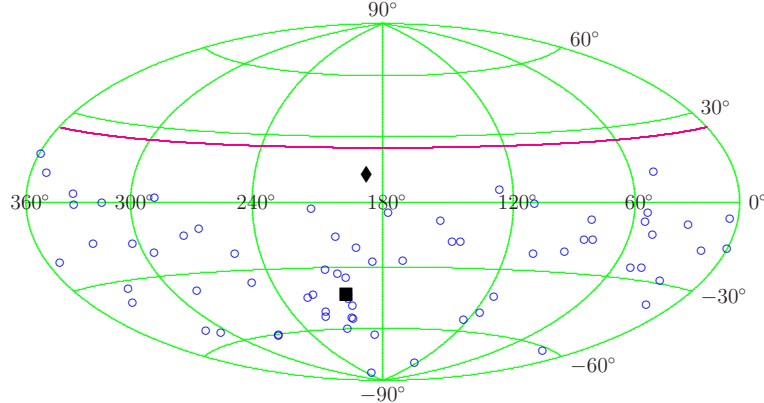


FIG. 1. Distribution of the arrival directions of 69 UHECR, represented by blue circles (\circ), with energy $E \geq 5.5 \times 10^{19}$ eV reported by PAO in 2010, in the equatorial coordinates plotted using the Hammer projection. The solid red line represents the exposure boundary of the PAO experiment. The locations of Centaurus A (\blacksquare) and M87 (\blacklozenge) are also shown for reference.

that the correlation of UHECR arrival directions with their sources can be completely erased. The energy cut 5.5×10^{19} eV of the released data was chosen to be higher enough than the GZK cutoff so that their sources can be restricted within the GZK radius ~ 100 Mpc. This high value of the energy cut is good enough for correlation analysis. Thus, we use the full set of released PAO data for our analysis.

From the Cen A dominance model, the expected arrival direction distribution can be obtained through the simulation. As an illustration, we show the arrival direction distributions of 6,900 mock UHECR for two different values of the Cen A fraction, $f_C = 1.0$ and $f_C = 0.3$ with the same smearing angle $\theta_s = 30^\circ$ in Fig. 2. From the observed UHECR set and the mock UHECR set, we obtain the observed and the expected CADDs/FEVDs as described in Eqs. (6) and (7), and calculate the KP statistic using Eq. (8). To obtain the KP statistic with sufficient accuracy, we generate 10^6 mock UHECR events. Though we still have small fluctuations in the KP statistic for this number of mock events, the accuracy is enough for our purpose. Then, the probability is calculated by using Eq. (9). We also checked the probability by direct Monte-Carlo simulation for several cases and confirmed that the Eq. (9) is good enough.

Fig. 3 shows CADDs and their CPDs of the PAO data, the isotropic distribution, and two cases of the Cen A dominance model. Close examination of CADD and its CPD is quite useful for understanding the results of statistical analysis and what causes the discrepancy between the data and the prediction of the model. For a single source, CADD is simply the distribution of angular distances of all UHECR from the source. The CADD of the isotropic distribution has a bell shape, reflecting the relative location of Cen A and the exposure function of the PAO experiment. On the contrary, the CADD of the PAO data has a distinguished peak at small angles, which means that there is an excess of observed UHECR near Cen A compared to the isotropic distribution. The KP test on CADD indicates that the probability that this excess of the PAO data is obtained from the isotropic distribution by chance is 1.3×10^{-3} . Thus, this excess can be attributed to the Cen A contribution.

The Cen A dominance model has two parameters, the Cen A fraction f_C and the smearing angle θ_s , which can be used to fit this excess peak and the remaining bell-shaped body. The Cen A fraction f_C affects the height of the peak at small angles relative to the bell-shaped

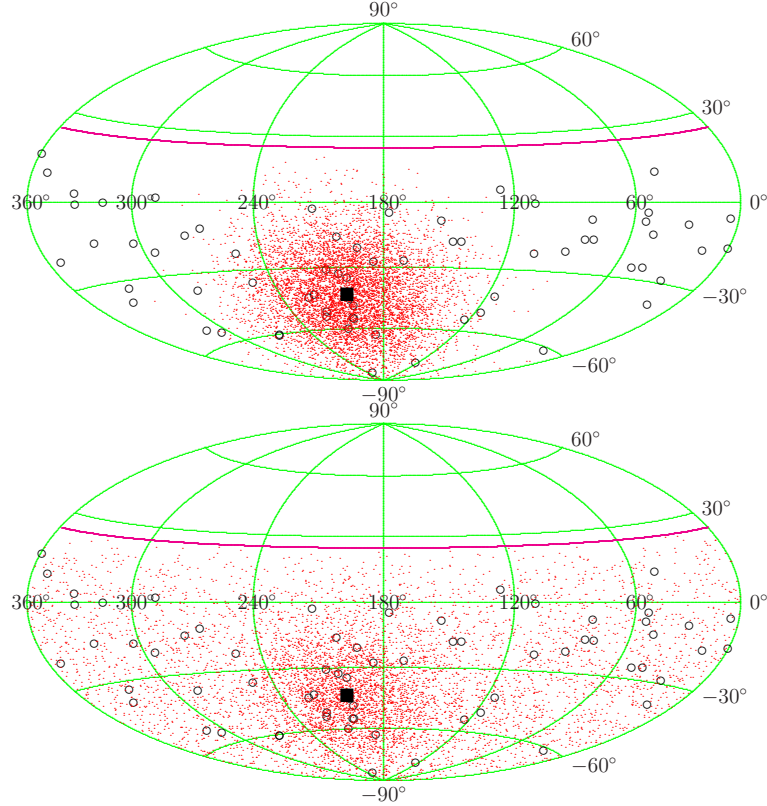


FIG. 2. Distributions of the mock UHECR arrival directions (6900 events, represented by small red dots) for the PAO experiment, obtained from the Cen A dominance model for two different values of the Cen A fraction $f_C = 1.0$ and $f_C = 0.3$ with the smearing angle $\theta_s = 30^\circ$.

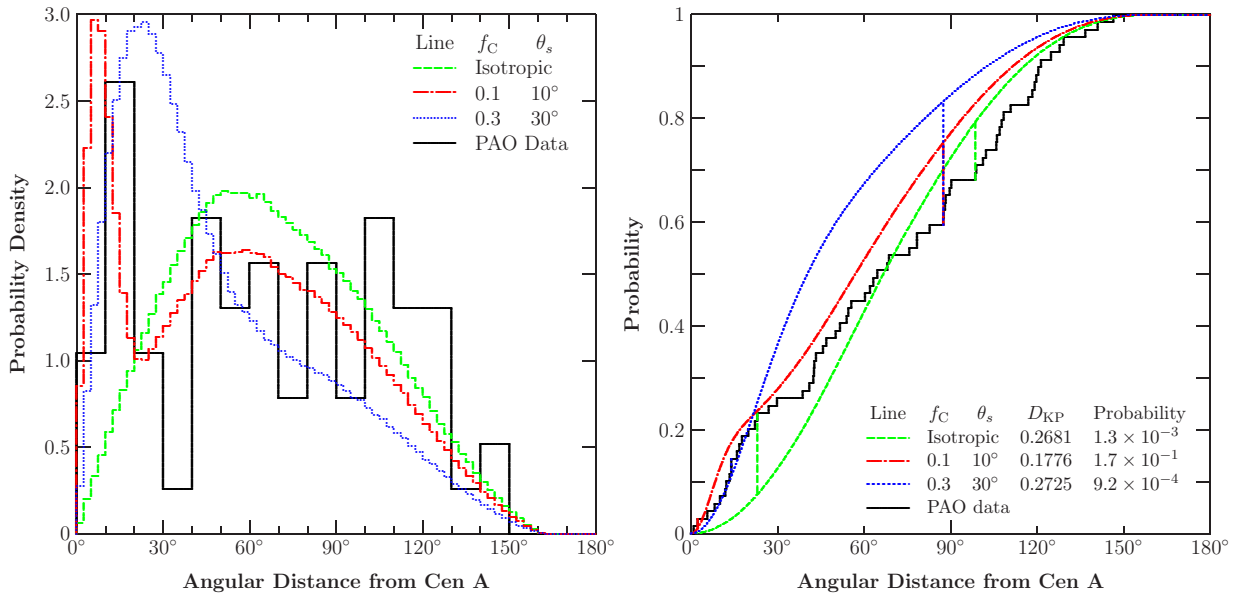


FIG. 3. CADDs (left panel) and their CPDs (right panel) of the PAO data, the isotropic distribution, and the Cen A dominance model with the parameter sets ($f_C = 0.1$, $\theta_s = 10^\circ$) and ($f_C = 0.3$, $\theta_s = 30^\circ$). Vertical lines in the right panel represent the sizes and the locations of the maximum differences between the CPD of the PAO data and those of the models considered.

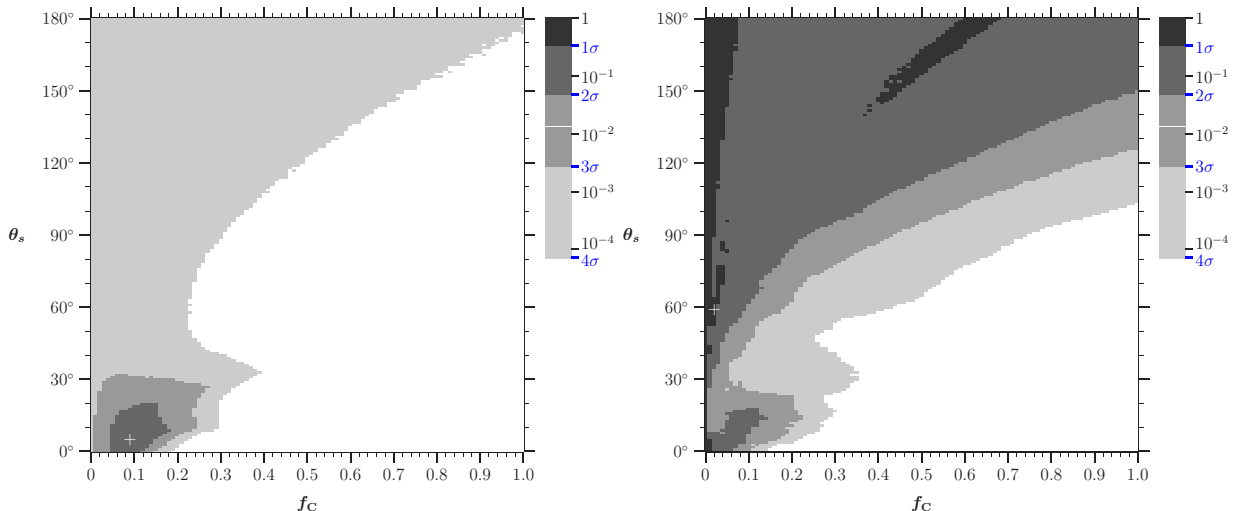


FIG. 4. Cen A fraction (f_C) and smearing angle (θ_s) dependence of probabilities that CADD (left panel) and FEVD (right panel) of the PAO data are obtained from the Cen A dominance model. The white + marks the parameter values of the maximum probability.

body at larger angles. The smearing angle θ_s changes the position and width of the peak. As θ_s increases, the Cen A contribution tends to be isotropic and the peak merges into the bell-shaped body. Fig. 4 shows the probability that CADD or FEVD of the observed PAO data is obtained from the Cen A dominance model, as a function of two parameters f_C and θ_s . Compared to the CADD method, the FEVD method seems to becomes rather insensitive for small Cen A fraction or large smearing angles where the distribution tends to be isotropic. At angles smaller than 30°, both the CADD and the FEVD methods give the similar and consistent results. Thus, we mainly use the results of the CADD method to extract our conclusions. For the CADD method, the best fit parameters at which the probability reaches its maximum value are $f_C \approx 0.1$ and $\theta_s = 5^\circ$, giving the maximum probability $P_{\max} = 0.29$. We don't have the 1σ band ($P \geq 0.32$) in the whole parameter ranges. However, this is not so disappointing, considering the simplicity of the Cen A dominance model that the distribution of UHECR which are not contributed by Cen A is assumed to be isotropic. As you can notice from the CPDs in Fig. 3, the parameters in the 2σ band fit the CPD at small angles well, but fitting gets poor at large angles where the isotropic contribution dominates. This makes the over-all fitting a little bit poor. The main cause of this poor fit is the big dip observed at angles 30°–40°, as seen in the CADD of the PAO data in Fig. 3. The big dip means the void region of UHECR at angular distance 30°–40° from Cen A, which is actually observed at the lower right region near the south pole in the skymap of Fig. 1. This departure from isotropy due to the void region makes the assumption of isotropic background in the Cen A dominance model a little bit poor one, though it is still a valid first approximation. Actually, this makes the best fit value of the smearing angle smaller than the naively (or more appropriately) expected value 10°–20° at which the peak of CADD is observed. Considering this uncertainty concerning the assumption of isotropic background, we extend the viable parameter range for the Cen A dominance model to the parameter range of 2σ band ($P \geq 0.046$): $0.05 \lesssim f_C \lesssim 0.15$ and $0^\circ \lesssim \theta_s \lesssim 20^\circ$. In Section II, we mentioned that f_C is different from $f_{C,PAO}$, the fraction of Cen A contribution as observed at the PAO experiment. Because Cen A is located at

the central region of the PAO exposure, $f_{C,PAO}$ is large than f_C . $f_{C,PAO}$ can be obtained as a function of f_C and θ_s when we do the Monte-Carlo simulation. In terms of $f_{C,PAO}$, the best-fit value is $f_{C,PAO} = 0.15$ and the 2σ band is $0.09 \lesssim f_{C,PAO} \lesssim 0.25$, which means that among 69 UHECR observed by PAO, about 10 (2σ band is $6 \sim 17$) UHECR can be attributed to Cen A contribution.

V. DISCUSSION AND CONCLUSION

Let us discuss the implications of the results obtained in the previous section. First of all, though we started with the hypothesis that Cen A is a dominant source of UHECR, what we can actually prove through our statistical analysis is that there is a strong source of UHECR in the direction of Cen A. To confirm that the actual source is Cen A, other evidences, e.g., from the acceleration mechanism, energetics, or the energy spectrum, are needed.

As seen in the previous section, the major source of uncertainty in our statistical analysis is the assumption that the background contribution is isotropic. We used the UHECR data with energies larger than 5.5×10^{19} eV, which is larger than the GZK cutoff. Thus, their sources are believed to be mostly located within the GZK radius ~ 100 Mpc, where the matter distribution is not isotropic. One important issue in the UHECR arrival directions is whether the UHECR sources trace the matter distribution. In this regard, it is important to check the existence of the correlation between the UHECR arrival directions and the matter distribution within the GZK radius. There have been several studies on this, and the existence of correlation is not yet conclusive [8–10]. Thus, we stick to the isotropic background instead of modeling the matter-tracing background. Concerning the background contribution, we again draw your attention to the fact that the CADD of the PAO data depicted in Fig. 3 shows the large deficit at 30° - 40° bin and another excess at 100° - 130° range compared to the isotropic distribution. The deficit is due to the void region near the south pole in the PAO data. The chance probability that this void region is obtained from the isotropic distribution is about 5.0×10^{-3} by the same CADD method and KP test. Not only the excess in the Cen A direction but also this void region makes the PAO data anisotropic. Another excess may be due to another point sources. We have examined the possibility of the existence of another point source at the region of angular distance 100° - 130° from Cen A, but found that this excess is consistent with isotropy.

The importance of searching for the point sources of UHECR is that it is the starting point of cosmic ray astronomy. A known point source of UHECR can be used to probe the intergalactic magnetic fields in the vicinity of the source. For Cen A, this kind of study was done in Ref. [26]. Here, we provide the order estimate from our results for comparison. Once we accept the results in the previous section that the fraction $f_{C,PAO} = 0.15$ of the observed UHECR by PAO is contributed by Cen A and their average deflection angle is around 10° , we can estimate the rms magnitude of the magnetic fields in the vicinity of Cen A. If we assume that the intergalactic magnetic field is composed of random patches of magnetic fields, the rough estimate for the deflection angle is given by [1]

$$\delta\theta = 0.8^\circ Z \left(\frac{E}{10^{20} \text{ eV}} \right)^{-1} \left(\frac{d\ell_c}{10 \text{ Mpc}^2} \right)^{1/2} \left(\frac{B}{10^{-9} \text{ G}} \right), \quad (10)$$

where E is the energy of the cosmic ray particle, d is the size of the magnetic field extension, ℓ_c is the average size of patches, and B is the magnetic field strength. If we select 10 nearest

UHECR from Cen A, the average energy is $E \sim 7.0 \times 10^{19}$ eV, and the average deflection angle is $\delta\theta \sim 10^\circ$ (The maximum deflection angle is $\delta\theta \sim 15^\circ$.). Inserting these values, $Z = 1$ (the proton), and the distance $d \sim 4$ Mpc, we obtain an estimate $B \sim 14 (\ell_c/\text{Mpc})^{-1/2}$ nG. This gives the rough strength of the intergalactic magnetic field in the vicinity of Cen A.

In conclusion, we examined the possibility that Cen A is a dominant source of UHECR observed by PAO, by using the statistical analysis of the arrival direction distribution. We set up the Cen A dominance model for the UHECR sources, in which Cen A contributes the fraction f_C of the whole UHECR with energy above 5.5×10^{19} eV and the isotropic background contributes the remaining $1-f_C$ fraction. The effect of the intergalactic magnetic fields on the bending of the trajectory of UHECR originated from Cen A is parameterized by the gaussian smearing angle θ_s . We adopted CADD and FEVD methods for the reduction of the arrival direction distribution, and the KP test to compare the observed and the expected CADD and FEVD and to estimate the significance level of the similarity. We observed the excess of UHECR in the Cen A direction in CADD. Then we tried to fit the CADD of the PAO data by varying two parameters f_C and θ_s of the Cen A dominance model. The best-fit parameter values are $f_C \approx 0.1$ ($f_{C,\text{PAO}} \approx 0.15$) and $\theta_s = 5^\circ$ with the probability $P = 0.29$. Considering the uncertainty concerning the assumption of isotropic background in the Cen A dominance model, we extend the viable parameter ranges to the 2σ band, $0.09 \lesssim f_{C,\text{PAO}} \lesssim 0.25$ and $0^\circ \lesssim \theta_s \lesssim 20^\circ$. It supports the existence of a point source in the direction of Cen A, which is extended by the action of intergalactic magnetic fields. If Cen A is actually the source responsible for the observed excess, the intergalactic magnetic field in the vicinity of Cen A is estimated to be $B \sim 14 (\ell_c/\text{Mpc})^{-1/2}$ nG from the average deflection angle of the excess UHECR.

ACKNOWLEDGMENT

This research was supported by Basic Science Research Program through the National Research Foundation (NRF) funded by the Ministry of Education, Science and Technology (2011-0002617).

-
- [1] M. Nagano and A. A. Watson, “Observations and implications of the ultrahigh-energy cosmic rays,” Rev. Mod. Phys. **72**, 689 (2000).
 - [2] J. Abraham *et al.* [Pierre Auger Collaboration], “Observation of the suppression of the flux of cosmic rays above 4×10^{19} eV,” Phys. Rev. Lett. **101**, 061101 (2008) [arXiv:0806.4302 [astro-ph]].
 - [3] R. U. Abbasi *et al.* [HiRes Collaboration], “Observation of the GZK cutoff by the HiRes experiment,” Phys. Rev. Lett. **100**, 101101 (2008) [arXiv:astro-ph/0703099].
 - [4] T. Abu-Zayyad, R. Aida, M. Allen, R. Anderson, R. Azuma, E. Barcikowski, J. W. Belz and D. R. Bergman *et al.*, “The Cosmic Ray Energy Spectrum Observed with the Surface Detector of the Telescope Array Experiment,” arXiv:1205.5067 [astro-ph.HE].
 - [5] P. Abreu *et al.* [Pierre Auger Observatory Collaboration], “Update on the correlation of the highest energy cosmic rays with nearby extragalactic matter,” Astropart. Phys. **34**, 314 (2010) [arXiv:1009.1855 [astro-ph.HE]].

- [6] J. Abraham *et al.* [Pierre Auger Collaboration], “Correlation of the highest energy cosmic rays with nearby extragalactic objects,” *Science* **318**, 938 (2007) [arXiv:0711.2256 [astro-ph]].
- [7] J. Abraham *et al.* [Pierre Auger Collaboration], “Correlation of the highest-energy cosmic rays with the positions of nearby active galactic nuclei,” *Astropart. Phys.* **29**, 188 (2008) [Erratum-*ibid.* **30**, 45 (2008)] [arXiv:0712.2843 [astro-ph]].
- [8] H. Takami, T. Nishimichi and K. Sato, “Systematic Survey of the Correlation between Northern HEGR Events and SDSS Galaxies,” arXiv:0910.2765 [astro-ph.HE].
- [9] A. J. Cuesta and F. Prada, “The correlation of UHECR with nearby galaxies in the Local Volume,” arXiv:0910.2702 [astro-ph.HE].
- [10] H. B. J. Koers and P. Tinyakov, “Testing large-scale (an)isotropy of ultra-high energy cosmic rays,” *JCAP* **0904**, 003 (2009). [arXiv:0812.0860 [astro-ph]].
- [11] H. Takami, T. Nishimichi, K. Yahata and K. Sato, “Cross-Correlation between UHECR Arrival Distribution and Large-Scale Structure,” *JCAP* **0906**, 031 (2009) [arXiv:0812.0424 [astro-ph]].
- [12] T. Kashti and E. Waxman, “Searching for a Correlation Between Cosmic-Ray Sources Above 10^{19} eV and Large-Scale Structure,” *JCAP* **0805**, 006 (2008) [arXiv:0801.4516 [astro-ph]].
- [13] R. U. Abbasi *et al.*, “Search for Correlations between HiRes Stereo Events and Active Galactic Nuclei,” *Astropart. Phys.* **30**, 175 (2008) [arXiv:0804.0382 [astro-ph]].
- [14] R. U. Abbasi *et al.* [HiRes Collaboration], “Search for Cross-Correlations of Ultra-High-Energy Cosmic Rays with BL Lacertae Objects,” *Astrophys. J.* **636**, 680 (2006) [arXiv:astro-ph/0507120].
- [15] G. E. Romero, J. A. Combi, L. A. Anchordoqui and S. .E. Perez Bergliaffa, “A possible source of extragalactic cosmic rays with arrival energies beyond the GZK cutoff,” *Astropart. Phys.* **5**, 279 (1996) [gr-qc/9511031].
- [16] L. A. Anchordoqui, H. Goldberg and T. J. Weiler, “An Auger test of the Cen A model of highest energy cosmic rays,” *Phys. Rev. Lett.* **87**, 081101 (2001) [astro-ph/0103043].
- [17] C. Isola, M. Lemoine and G. Sigl, “Centaurus A as the source of ultrahigh-energy cosmic rays?,” *Phys. Rev. D* **65**, 023004 (2002) [astro-ph/0104289].
- [18] M. J. Hardcastle, C. C. Cheung, I. J. Feain and L. Stawarz, “High-energy Particle Acceleration and Production of Ultra-high-energy Cosmic Rays in the Giant Lobes of Centaurus A,” *Mon. Not. Roy. Astron. Soc.* **393**, 1041 (2009) [arXiv:0808.1593 [astro-ph]].
- [19] M. Honda, “Ultra-High Energy Cosmic-Ray Acceleration in the Jet of Centaurus A,” *Astrophys. J.* **706**, 1517 (2009) [arXiv:0911.0921 [astro-ph.HE]].
- [20] Gopal-Krishna, P. L. Biermann, V. de Souza and P. J. Wiita, “Ultra-High Energy Cosmic Rays from Centaurus A: Jet Interaction with Gaseous Shells,” arXiv:1006.5022 [astro-ph.HE].
- [21] N. Fraija, S. Sahu and B. Zhang, “Very High Energy Cosmic Rays from Centaurus A,” arXiv:1007.0455 [hep-ph].
- [22] L. A. Anchordoqui, H. Goldberg and T. J. Weiler, “Update on tests of the Cen A neutron-emission model of highest energy cosmic rays,” *Phys. Rev. D* **84**, 067301 (2011) [arXiv:1103.0536 [astro-ph.HE]].
- [23] H. B. Kim and J. Kim, “Statistical Analysis of the Correlation between Active Galactic Nuclei and Ultra-High Energy Cosmic Rays,” *JCAP* **1103**, 006 (2011) [arXiv:1009.2284 [astro-ph.HE]].
- [24] H. B. Kim and J. Kim, “Update of Correlation Analysis between Active Galactic Nuclei and Ultra-High Energy Cosmic Rays,” arXiv:1203.0386 [astro-ph.HE].
- [25] G. L. H. Harris, M. Rejkuba and W. E. Harris, “The Distance to NGC 5128 (Centaurus A),” *Publ. Astron. Soc. Austral.* **27**, 457 (2010) [arXiv:0911.3180 [astro-ph.GA]].

- [26] H. Yuksel, T. Stanev, M. D. Kistler and P. P. Kronberg, “The Centaurus A Ultrahigh-Energy Cosmic Ray Excess and the Local Extragalactic Magnetic Field,” arXiv:1203.3197 [astro-ph.HE].